

Correlation between the charge radii difference in mirror partner nuclei and the symmetry energy slope

Xiao-Rong Ma,¹ Shuai Sun,² Rong An,^{1,2,*} and Li-Gang Cao^{2,3,†}

¹*School of Physics, Ningxia University, Yinchuan 750021, China*

²*Key Laboratory of Beam Technology of Ministry of Education,*

College of Nuclear Science and Technology, Beijing Normal University, Beijing 100875, China

³*Key Laboratory of Beam Technology of Ministry of Education, Institute of Radiation Technology, Beijing Academy of Science and Technology, Beijing 100875, China*

(Dated: April 16, 2024)

Correlation between the charge radii difference of mirror partner nuclei ΔR_{ch} and the slope parameter L of symmetry energy has been built to ascertain the equation of state of isospin asymmetric nuclear matter. In this work, the influence of pairing correlations and isoscalar compression modulus on the ΔR_{ch} are systematically investigated by Skyrme density functionals theory. The calculated results suggest that the linear correlation between ΔR_{ch} and L is decreased by the surface pairing correlations. The slope parameter deduced from the difference of charge radii of mirror-pair nuclei ^{32}Ar - ^{32}Si , ^{36}Ca - ^{36}S , ^{38}Ca - ^{38}Ar , and ^{54}Ni - ^{54}Fe falls into the range of $L = 42.57$ - 50.64 MeV, namely the rather soft equation of state of asymmetric nuclear matter. Besides, the range of slope parameter can also be influenced by the effective forces classified by various isoscalar incompressibility coefficients.

I. INTRODUCTION

Nuclear symmetry energy can be generally employed to comprehend the underlying physical mechanism from the terrestrial nuclei to dense astrophysical events [1–6]. So far, plenty of methods are undertaken to constrain the nuclear symmetry energy, such as the extracted neutron skin thickness (NST) [7–12], properties of giant resonances [13–17], quantities of the heavy-ion collision [18–23], etc. However, a unified density-dependence of symmetry energy is hardly determined due to the uncertainties suffering from different theoretical models. Thus more alternative observables should be urgently required in constraining the equation of state (EoS) of asymmetric nuclear matter. The difference of charge radii of mirror-pair nuclei has been proposed as a tentative probe to evaluate the slope parameter of symmetry energy L [24, 25]. And then the precisely measured charge radii differences in mirror partner nuclei ^{32}Ar - ^{32}Si , ^{36}Ca - ^{36}S , ^{38}Ca - ^{38}Ar , and ^{54}Ni - ^{54}Fe are thereby used to validate the range of slope parameter L [26–28].

Charge radii differences in mirror pair nuclei are strongly associated with the neutron-skin thickness of neutron-rich nuclei and with the slope parameter L [24, 25]. As shown in Ref. [29], the calculations performed by relativistic energy density functionals (EDFs) further inspect the validity of this assumption. It points out that the difference in proton radii of mirror nuclei can be indeed employed to constrain the EoS of isospin asymmetric nuclear matter. This may provide an alternative approach to extract the content information about the neutron skin thickness as well [30]. Recent study suggests

that mirror-difference in nuclear charge radii is proportional to the isospin asymmetry $I = (N - Z)/A$, where N and Z represent the neutron and proton number of a nucleus, respectively, and $A = N + Z$ is the corresponding mass number [31]. Here the same scenario can also be observed between the difference of binding energy per nucleon of mirror nuclei and the Coulomb asymmetry. Furthermore, combing the accurately detected charge radii differences in mirror partner nuclei, the upper limit range of symmetry energy slope has been determined at $L \approx 100$ MeV [32].

Method mentioned above requires that more accurate charge radii data should be obtained through different nuclear models. With the improvement of experimental technique, high-precision charge radii of exotic nuclei can be possibly detected [33]. Thus more charge radii data of nuclei far away from the β -stability line are compiled [34, 35]. This provides a fundamental guideline for theoretical study to access the charge radii of mirror partner nuclei. A reliable description of nuclear charge radii is influenced by various mechanisms, such as shape deformation [36–39], pairing correlations [40–42], shell closure effects [43, 44], etc. As is well known, pairing correlations play an important role in describing the ground state properties of finite nuclei [45–47] or the quasiparticle resonant states [48]. Especially, it is mentioned that the radius of neutron-rich nuclei can also be influenced evidently by the pairing correlations [49].

As demonstrated in Ref. [50], pairing correlations should be taken into account in calculating the nuclear charge radii. Shown in Ref. [51], the density energy functionals consisting of Skyrme and covariant models are undertaken to systematically investigate the correlations between the charge radii differences in mirror partner nuclei and slope parameter L . The calculated results suggest the linear correlation between the mirror difference in charge radii and slope parameter L is further

* Corresponding author:rongan@nxu.edu.cn

† Corresponding author:caolg@bnu.edu.cn

decreased by considering the pairing effects. In contrast, the correlation between the neutron-skin thickness of a neutron-rich nucleus and the proton radii difference of the corresponding mirror nuclei is mostly enhanced by pairing effects [30]. Meanwhile, it is also mentioned that the compression modulus of symmetric nuclear matter has an influence on determining the slope parameter L [52].

The density-dependence of nuclear symmetry energy, which is mostly determined by the slope parameter L , is associated with the isovector-sensitive indicators in the EoS of isospin asymmetry systems. In Ref. [53], it suggests that the correlation between the isoscalar incompressibility K and the NST is not clear. Further study demonstrates that the correlations between K and the isovector parameters are generally weaker in comparison with the strong correlation between NST and symmetry energy coefficients [54, 55]. Actually, the nuclear matter properties recognizing the isoscalar and isovector counterparts are mutually correlated with the effective model parameters. This means the influence coming from the isoscalar sector is non-negligible in discussing the isovector properties [56, 57]. As suggested in Refs. [58–60], the compression modulus of symmetric nuclear matter is sensitive to the density dependence of symmetry energy. Therefore, it is also essential to investigate the correlation between the difference of charge radii of mirror-partner nuclei and the slope parameter L under various incompressibility coefficients K . In this work, the influence of pairing correlations and isoscalar compression modulus on the charge radii differences of mirror partner nuclei ^{32}Ar - ^{32}Si , ^{36}Ca - ^{36}S , ^{38}Ca - ^{38}Ar , and ^{54}Ni - ^{54}Fe are investigated by the spherical Skyrme EDFs. Furthermore, the range of slope parameter L deriving from the charge radii differences of mirror-pair nuclei is discussed as well.

The structure of the paper is organized as the follows. Sec. II is devoted to presenting the theoretical framework briefly. In Sec. III, the numerical results and discussion are provided. Finally, a summary and outlook is given in Sec. IV.

II. THEORETICAL FRAMEWORK

The sophisticated Skyrme-type energy density functional, which was expressed as an effective zero-range force between nucleons with density-dependent and momentum-dependent terms, has made remarkable success in describing various physical phenomena [48, 49, 61–75]. In general, the effective force sets have been determined by calibrating the properties of finite nuclei and symmetry nuclear matter at saturation density ρ_0 ($\approx 0.16 \text{ fm}^{-3}$). It is notably mentioned that the Skyrme EDF can give analytical expression of all variables characterizing infinite nuclear matter (see, e.g., [76, 77] for details). In this work, the Skyrme-like effective interac-

tion has been recalled as follows [78–80],

$$\begin{aligned}
 V(\mathbf{r}_1, \mathbf{r}_2) = & t_0(1 + x_0 \mathbf{P}_\sigma) \delta(\mathbf{r}) \\
 & + \frac{1}{2} t_1(1 + x_1 \mathbf{P}_\sigma) [\mathbf{P}'^2 \delta(\mathbf{r}) + \delta(\mathbf{r}) \mathbf{P}^2] \\
 & + t_2(1 + x_2 \mathbf{P}_\sigma) \mathbf{P}' \cdot \delta(\mathbf{r}) \mathbf{P} \\
 & + \frac{1}{6} t_3(1 + x_3 \mathbf{P}_\sigma) [\rho(\mathbf{R})]^\alpha \delta(\mathbf{r}) \\
 & + iW_0 \sigma \cdot [\mathbf{P}' \times \delta(\mathbf{r}) \mathbf{P}].
 \end{aligned} \tag{1}$$

Here, $\mathbf{r} = \mathbf{r}_1 - \mathbf{r}_2$ and $\mathbf{R} = (\mathbf{r}_1 + \mathbf{r}_2)/2$ are related to the positions of two nucleons \mathbf{r}_1 and \mathbf{r}_2 , $\mathbf{P} = (\nabla_1 - \nabla_2)/2i$ is the relative momentum operator and \mathbf{P}' is its complex conjugate acting on the left, and $\mathbf{P}_\sigma = (1 + \vec{\sigma}_1 \cdot \vec{\sigma}_2)/2$ is the spin exchange operator that controls the relative strength of the $S = 0$ and $S = 1$ channels for a given term in the two-body interactions, with $\vec{\sigma}_{1(2)}$ being the Pauli matrices. The last term represents the spin-orbit force where $\sigma = \vec{\sigma}_1 + \vec{\sigma}_2$. The quantities α , t_i and x_i ($i = 0-3$) represent the parameters of the Skyrme forces used in this work.

Solving the Schrödinger-like equations by the self-consistent iteration leads to the eigenenergies and wave functions of constituent nucleons. The pairing correlations can be generally treated either by the BCS method or by the Bogoliubov transformation [45, 46, 81]. In this work, spherical Skyrme Hartree-Fock-Bogoliubov (HFB) approach is utilized for all calculations [82]. The density-dependent zero-range pairing force is employed as follows [83],

$$V_{\text{pair}}(\mathbf{r}_1, \mathbf{r}_2) = V_0 \left[1 - \eta \left(\frac{\rho(\mathbf{r})}{\rho_0} \right) \right] \delta(\mathbf{r}_1 - \mathbf{r}_2), \tag{2}$$

where $\rho(\mathbf{r})$ is the baryon density in coordinate space and $\rho_0 = 0.16 \text{ fm}^{-3}$ represents the nuclear saturation density. The value of η is taken as 0.0, 0.5, or 1.0 for volume-, mixed-, or surface-type pairing interactions, respectively. The quantity V_0 is adjusted by calibrating the empirical pairing gaps with three-point formula [47, 83], and the values of V_0 are 188.2 MeV fm^3 , 370.2 MeV fm^3 and 509.6 MeV fm^3 for the corresponding volume-, mixed-, and surface-type pairing interactions, respectively.

After achieving the convergence of the total binding energy, the root-mean square (rms) radii of the neutron and proton matter, and the neutron-skin thickness can be obtained naturally. The quantity of nuclear charge radius (R_{ch}) can be calculated through (in units of fm^2)

$$R_{\text{ch}}^2 = \langle r_{\text{p}}^2 \rangle + 0.64 \text{ fm}^2. \tag{3}$$

The first term represents the charge density distributions of point-like protons and the second term is due to the finite size of protons [84]. For mirror pair nuclei, the difference in charge radii (ΔR_{ch}) can be obtained through the formula mentioned above.

The density dependence of symmetry energy can be

TABLE I. Parameters of the forces used in this work, where the parameter $\alpha = 1/6$. Saturation properties of the Skyrme parametrization sets used in this work, such as the incompressibility coefficients K (MeV), slope parameter L (MeV) and symmetry energy E_{sys} (MeV) at saturation density ρ_0 (fm^{-3}), are also shown.

K	Sets	t_0	t_1	t_2	t_3	x_0	x_1	x_2	x_3	W_0	L	E_{sys}
$K \approx 230$	s3028	-2461.903	472.082	-530.239	13599.53	1.6830	-0.3349	-1.0	2.6602	124.766	-11.2262	28
	s3030	-2477.013	475.604	-533.657	13709.09	1.1408	-0.3365	-1.0	1.8302	117.482	22.8715	30
	s3032	-2491.849	486.614	-579.661	13842.35	0.9962	-0.2791	-1.0	1.5763	128.028	36.2246	32
	s3034	-2503.455	489.112	-591.648	13939.40	0.7308	-0.2622	-1.0	1.1527	126.846	56.1442	34
	s3036	-2513.951	491.018	-615.662	14045.31	0.5457	-0.2210	-1.0	0.8437	128.528	71.5428	36
	s3038	-2524.594	494.060	-635.510	14142.73	0.3550	-0.1916	-1.0	0.5315	129.200	87.6155	38
	s3040	-2531.688	489.598	-625.976	14203.48	0.1249	-0.1940	-1.0	0.1662	122.045	106.0862	40
$K \approx 240$	s4028	-2296.534	515.586	-336.464	11786.33	1.7714	-0.8491	-1.0	3.1703	118.803	3.9774	28
	s4030	-2317.546	532.898	-355.019	11907.07	1.2924	-0.8449	-1.0	2.3824	118.263	34.0735	30
	s4032	-2321.087	520.235	-491.504	12164.33	1.2626	-0.5755	-1.0	2.1916	136.989	34.4283	32
	s4034	-2329.794	510.932	-423.708	12179.54	0.8546	-0.6759	-1.0	1.5447	117.932	62.5884	34
	s4036	-2337.516	507.834	-424.568	12253.22	0.7156	-0.6664	-1.0	1.2882	118.414	75.6679	36
	s4038	-2355.765	523.051	-465.145	12389.16	0.3790	-0.6244	-1.0	0.7299	118.238	98.6522	38
	s4040	-2359.001	513.325	-475.563	12466.46	0.2959	-0.5827	-1.0	0.5558	119.406	108.1741	40
$K \approx 250$	s5028	-2157.179	599.608	-396.271	10352.38	1.4017	-0.9193	-1.0	2.9016	138.874	33.0037	28
	s5030	-2155.199	570.378	-299.172	10324.29	1.6366	-1.0334	-1.0	3.2711	131.218	30.0248	30
	s5032	-2172.510	583.512	-348.992	10472.92	1.4649	-0.9688	-1.0	2.9140	141.589	43.5871	32
	s5034	-2179.610	584.069	-331.053	10501.79	1.2593	-0.9977	-1.0	2.5371	141.094	60.3202	34
	s5036	-2195.402	599.442	-365.556	10609.25	0.9683	-0.9629	-1.0	2.0020	145.638	80.1762	36
	s5038	-2205.358	602.093	-375.998	10690.19	0.7284	-0.9493	-1.0	1.5517	145.124	97.4925	38
	s5040	-2214.249	600.714	-404.383	10802.96	0.5278	-0.9019	-1.0	1.1569	146.358	112.2079	40

expanded around the saturation density ρ_0 as follows

$$E_{\text{sys}}(\rho) \approx E_{\text{sys}}(\rho_0) + \frac{L}{3} \left(\frac{\rho - \rho_0}{\rho_0} \right) + \frac{K_{\text{sym}}}{18} \left(\frac{\rho - \rho_0}{\rho_0} \right)^2 + \dots, \quad (4)$$

where L and K_{sym} are the slope and curvature of symmetry energy at nuclear saturation density ρ_0 , respectively. These two quantities are defined as

$$L = 3\rho_0 \left. \frac{\partial E_{\text{sys}}(\rho)}{\partial \rho} \right|_{\rho=\rho_0}, \quad (5)$$

$$K_{\text{sym}} = 9\rho_0^2 \left. \frac{\partial^2 E_{\text{sys}}(\rho)}{\partial \rho^2} \right|_{\rho=\rho_0}. \quad (6)$$

Also, the isoscalar incompressibility K of symmetric nuclear matter is recalled as

$$K = 9\rho_0^2 \left. \frac{\partial^2 E_0(\rho)}{\partial \rho^2} \right|_{\rho=\rho_0}. \quad (7)$$

Here, the quantity $E_0(\rho)$ is the energy per particle of symmetric nuclear matter [30]. The nuclear incompressibility can be extracted from the measurements of the isoscalar giant monopole resonance (ISGMR) in medium-heavy nuclei [83, 85]. In addition, it is also mentioned that the incompressibility of symmetric nuclear matter can be deduced from the α -decay properties [86]. In Table I, parameters of the Skyrme forces used in this work are shown. The corresponding saturation properties in infinite nuclear matter derived from the Skyrme forces, such as isoscalar incompressibility K , slope parameter L , and symmetry energy E_{sys} , are also shown explicitly. Both the slope parameter L and symmetry energy E_{sys} at saturation density cover a wide range.

III. RESULTS AND DISCUSSION

Linear correlation between the charge radii differences in the mirror partner nuclei ^{32}Ar - ^{32}Si , ^{36}Ca - ^{36}S , ^{38}Ca - ^{38}Ar , and ^{54}Ni - ^{54}Fe and the slope parameter of symmetry energy has been sequentially employed to constrain the equation of state of isospin asymmetric nuclear matter [26–28]. In Table II, the experimental data of R_{ch}

TABLE II. R_{ch} and ΔR_{ch} database for the $A = 32, 36, 38$ and 54 mirror-pair nuclei. The parentheses on the values of charge radii and the difference of charge radii are shown with systematic uncertainties [26–28, 34, 87].

A		R_{ch} (fm)	ΔR_{ch} (fm)
32	Ar	3.3468(62)	
	Si	3.153(12)	0.194(14)
36	Ca	3.4484(27)	
	S	3.2982(12)	0.150(4)
38	Ca	3.4652(17)	
	Ar	3.4022(15)	0.063(3)
54	Ni	3.7370(30)	
	Fe	3.6880(17)	0.049(4)

and ΔR_{ch} for $A = 32, 36, 38$ and 54 mirror-pair nuclei are given. As mentioned above, nuclear charge radius is influenced by the pairing correlations [40–42]. Thus the influence on the correlations between the charge radii difference in mirror partner nuclei and the slope parameter L should be systematically investigated.

In Fig. 1, plots for charge radii difference ΔR_{ch} in ^{54}Ni - ^{54}Fe against symmetry energy slope L are depicted by various pairing forces. For the convenience of discussion,

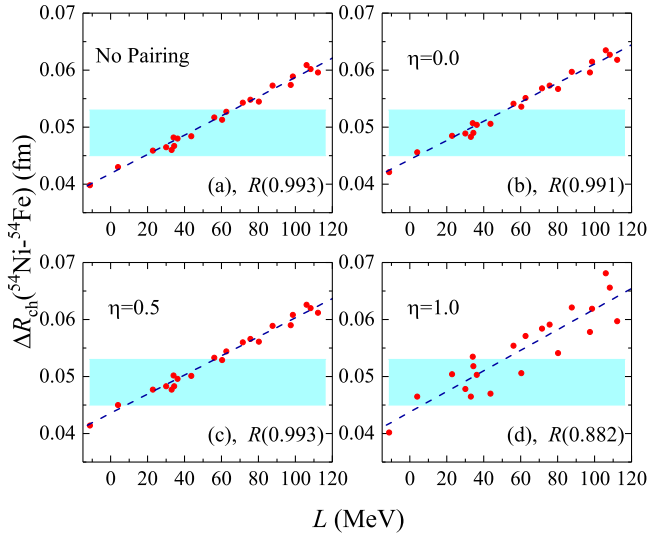


FIG. 1. (Color online) Charge radii difference ΔR_{ch} of mirror partner nuclei ^{54}Ni - ^{54}Fe as a function of slope parameter L is depicted under various pairing forces, e.g., no pairing (a), volume type $\eta = 0.0$ (b), mixed type $\eta = 0.5$ (c) and surface type $\eta = 1.0$ (d) pairing forces. The Pearson coefficients R are given in the parenthesis. The database takes from Refs. [27, 34, 35] and the symmetric error bands are labeled by light blue.

the Pearson coefficient R , which is used to measure the degree of correlation between two variables, is employed in our study. Without considering the pairing correlations, the Pearson coefficient R between ΔR_{ch} of mirror partner nuclei ^{54}Ni - ^{54}Fe and L is given to be 0.993. The same scenario can also be found in mixed-type pairing forces. For the volume-type pairing force, the Pearson coefficient R is almost equivalent to no pairing and $\eta = 0.0$ cases. As demonstrated in Ref. [51], the linear correlation between ΔR_{ch} and L is decreased by the pairing effects. From Fig. 1, one can find that the surface-type pairing force actually decrease the linear correlation between ΔR_{ch} and L in mirror pair nuclei ^{54}Ni - ^{54}Fe , in which the Pearson coefficient R falls into 0.882. Actually, more particles are scattered into the higher single levels under the surface pairing force. This leads to the rather poor correlation between the difference of charge radii of mirror partner nuclei and the slope parameter L .

For further focusing on the linear correlation between ΔR_{ch} and L , charge radii differences ΔR_{ch} of mirror partner nuclei ^{32}Ar - ^{32}Si , ^{36}Ca - ^{36}S , and ^{38}Ca - ^{38}Ar against slope parameter L are shown in Fig. 2. In this figure, clear linear correlations can be observed for these mirror-pair nuclei ^{32}Ar - ^{32}Si , ^{36}Ca - ^{36}S , and ^{38}Ca - ^{38}Ar . For the volume-type pairing force, the Pearson coefficients are almost no change in the mirror partner nuclei ^{32}Ar - ^{32}Si , ^{36}Ca - ^{36}S and ^{38}Ca - ^{38}Ar , namely the corresponding R values are 0.926, 0.881 and 0.836, respectively. With considering the mixed-type pairing force, the Pearson coefficients R are slightly improved with respect to the no

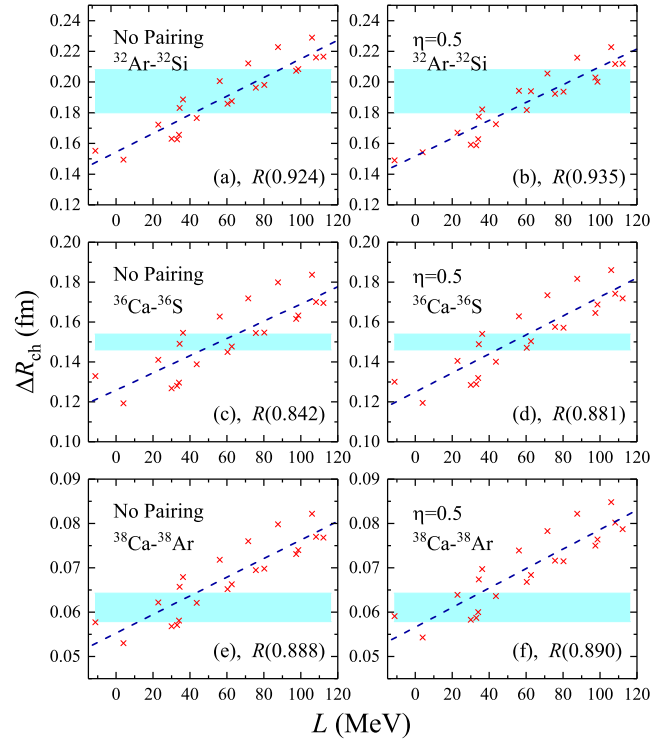


FIG. 2. (Color online) Charge radii differences ΔR_{ch} of mirror partner nuclei ^{32}Ar - ^{32}Si , ^{36}Ca - ^{36}S , and ^{38}Ca - ^{38}Ar as a function of slope parameter L are depicted under no pairing and mixed-type $\eta = 0.5$ pairing forces. The Pearson coefficients R are given in the parenthesis. The database takes from Refs. [26, 28, 34, 35] and the symmetric error bands are labeled by light blue.

pairing case. Actually, the Pearson coefficients R are rather poor if the surface pairing force is taken into account. Here the corresponding figures are not shown, but the Pearson coefficients R with considering surface-type pairing force are 0.887, 0.791 and 0.743 for the corresponding mirror partner nuclei ^{32}Ar - ^{32}Si , ^{36}Ca - ^{36}S and ^{38}Ca - ^{38}Ar , respectively. This means that pairing effect can decrease the linear correlation between ΔR_{ch} and L if the pairing interactions are only tackled by the surface-type pairing force.

As mentioned in Refs. [24–28], charge radii differences in mirror partner nuclei provide an alternative approach to pin down the isovector components in the equation of state of asymmetric nuclear matter. To facilitate the relatively clear linear correlation between ΔR_{ch} and L , the mixed-type pairing force is employed in the following discussion. In Fig. 3, the deduced slope parameters L from the differences of charge radii of mirror-pair nuclei ^{54}Ni - ^{54}Fe , ^{38}Ca - ^{38}Ar , ^{36}Ca - ^{36}S , and ^{32}Ar - ^{32}Si are drawn by shaping the covered range in Fig. 2. Combing the experimental data, the extracted slope parameter falls into the range of $L = 42.57$ - 50.64 MeV. From this figure, one can find that the deduced value of L covers the uncertainty range deriving from the mirror charge radii

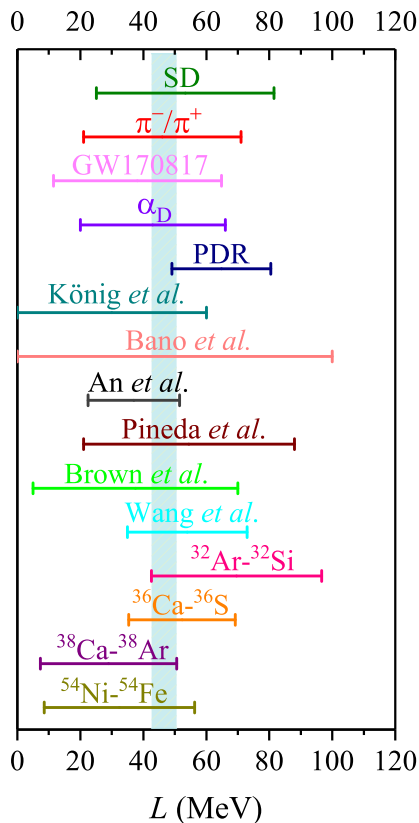


FIG. 3. (Color online) Plots for the values of slope parameter L extracted in this work (^{54}Ni - ^{54}Fe , ^{38}Ca - ^{38}Ar , ^{36}Ca - ^{36}S , and ^{32}Ar - ^{32}Si) and those from the existing literatures. The partially enumerated values of L , such as Wang *et al.* [24], Brown *et al.* [26], Pineda *et al.* [27], An *et al.* [88], Bano *et al.* [32], König *et al.* [28], pygmy dipole resonance (PDR) [89], electric dipole polarizability α_D [15], GW170817 [90], pion production (π^-/π^+) [91], and the charge exchange spin-dipole (SD) excitations [17], are also given. The color band represents the extracted slope parameter $L = 42.57$ - 50.64 MeV in this literature.

differences [24, 26–28, 32, 88]. Here it is mentioned that the upper limit range of L coming from ^{32}Ar - ^{32}Si is 96.65 MeV. This result is overestimated in comparison with the Ref. [28] where the upper range is confined to be $L \leq 60$ MeV. This may be due to the fact that shape deformation is ignored in our study. Besides, the pairing correlations and the limited Skyrme parameter sets used here may also have an influence on evaluating the interval range of slope parameter L .

Also, the value of symmetry energy slope L extracted from pygmy dipole resonance (PDR) locates at the internal range of $L = 64.8 \pm 15.7$ [89]. The covered range is very narrow with respect to other cases of this figure. Furthermore, the extracted L in this work can cover the uncertainty ranges deriving from the nuclear electric dipole polarizability α_D [15], dense astrophysical event GW170817 [90], the pion production ratios in heavy-ion collisions [91] and the charge exchange spin-dipole (SD)

excitations [17]. Besides, this deduced result can mostly cover the range of L shown in Ref. [92], in which the slope parameter captures the range of $L = 47.3 \pm 7.8$. In a word, the extracted range of slope parameter $L = 42.57$ - 50.64 MeV means that the rather soft equation of state of isospin asymmetric nuclear matter can be obtained from the implication of charge radii difference in mirror-pair nuclei.

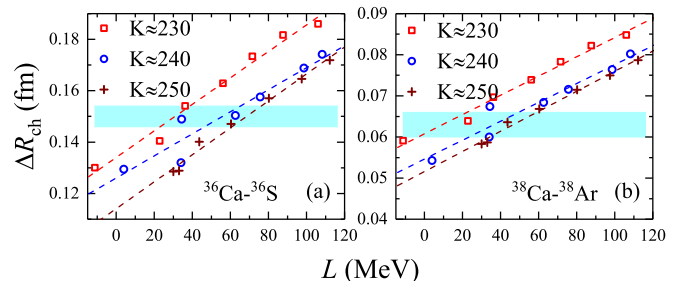


FIG. 4. (Color online) Charge radii differences ΔR_{ch} of mirror partner nuclei ^{36}Ca - ^{36}S and ^{38}Ca - ^{38}Ar are plotted as a function of slope parameter L classified by various isoscalar incompressibility coefficients K . The corresponding experimental data are taken from Ref. [26].

As shown in Fig. 2, the Pearson coefficients become lower for the mirror-pair nuclei ^{36}Ca - ^{36}S and ^{38}Ca - ^{38}Ar . This suggests that the profoundly theoretical uncertainties are encountered in the calibrating protocol. In order to clarify this phenomenon, the charge radii differences ΔR_{ch} of mirror partner nuclei ^{36}Ca - ^{36}S and ^{38}Ca - ^{38}Ar against the slope parameter L classified by various isoscalar incompressibility coefficients K are shown in Fig. 4. From both panels of Fig. 4, one can find that the isoscalar incompressibility has an influence on the charge radii difference of mirror partner nuclei. Even from $K \approx 230$ to $K \approx 250$ MeV, the deviated range for L is about 38.0 MeV. Here, as shown in Fig. 3, we mention that the influence of the isoscalar incompressibility coefficient cannot be taken into account in evaluating the slope parameter L . Significantly the isoscalar incompressibility may be indispensable in calibrating protocol. As is well known, the accurate description of the density-dependent behavior of symmetry energy plays an important role in recognizing various physical mechanisms through nuclear models, such as the production of superheavy elements [93], and the cluster radioactivity [94, 95], etc. Especially, recent study suggests that the effective proton-neutron chemical potential difference of neutron-rich nuclei is strongly sensitive to the symmetry energy [96]. Therefore, more aspects should be taken into account in constraining the slope parameter L .

IV. SUMMARY AND OUTLOOK

In this work, the correlation between the charge radii differences (ΔR_{ch}) in mirror-pair nuclei ^{32}Ar - ^{32}Si , ^{36}Ca -

^{36}S , ^{38}Ca - ^{38}Ar , and ^{54}Ni - ^{54}Fe and slope parameter L at saturation density is investigated by the spherical Skyrme energy density functionals. The calculated results suggest that the surface pairing force can further decrease the linear correlation between ΔR_{ch} and L . The deduced slope parameter locates the interval range of $L = 42.57$ - 50.64 MeV under the mixed pairing interaction, namely the rather soft equation of state. This is in accord with most existing literatures. Meanwhile, the influence of isoscalar nuclear matter property on ΔR_{ch} is inevitable in constraining the nuclear matter EoS. This may suggest that most parametrization forces are ruled out in the calibrated procedure. As shown in Fig. 4, the correlation between charge radii difference of mirror nuclei and the slope parameter of symmetry energy is influenced by nuclear incompressibility. This seems to suggest that the Skyrme parameter sets adjusted to different slope parameters under specific incompressibility coefficient can give highly linear correlation between the charge radii difference of mirror partner nuclei and the slope parameter L . Meanwhile, this may provide an alternative approach to evaluate the possible influential quantities in determining the EoS of asymmetric nuclear matter. Shown in Ref. [51], the calculated results obtained by density energy functionals consisting of Skyrme and covariant models suggest that more mirror-pair nuclei are ruled out

in constraining the slope parameter L , but the superior candidates of mirror-pair nuclei ^{44}Cr - ^{44}Ca and ^{46}Fe - ^{46}Ca may be used to ascertain the limit range of L . Thus more discussion should be performed in the proceeding work.

Recently studies show that the charge-changing cross section measurements can be used to determine the EoS of nuclear matter with mirror nuclei [97]. This method can also be employed to investigate the charge radii of exotic nuclei [98] and the isospin interactions [99]. This provides an accessible approach to ascertain the nuclear symmetry energy. From the aspect of the charge radii difference in mirror-pair nuclei, the underlying mechanism should be taken into account in determining the nuclear symmetry energy, such as the local relations among the adjacent neighbouring nuclei [100–103], the α -cluster formation [104, 105], etc. Thus more high-precision charge radii data are urgently required in experimental and theoretical researches.

ACKNOWLEDGMENTS

This work is supported by the National Natural Science Foundation of China under Grants No. 12275025, No. 11975096 and the Fundamental Research Funds for the Central Universities (2020NTST06).

-
- [1] A. Steiner, M. Prakash, J. Lattimer, and P. Ellis, *Phys. Rept.* **411**, 325 (2005).
 - [2] B.-A. Li, L.-W. Chen, and C. M. Ko, *Phys. Rept.* **464**, 113 (2008).
 - [3] X. Roca-Maza and N. Paar, *Prog. Part. Nucl. Phys.* **101**, 96 (2018).
 - [4] F. Ji, J. Hu, S. Bao, and H. Shen, *Phys. Rev. C* **100**, 045801 (2019).
 - [5] Y. Zhang, M. Liu, C.-J. Xia, Z. Li, and S. K. Biswal, *Phys. Rev. C* **101**, 034303 (2020).
 - [6] J.-F. Xu, C.-J. Xia, Z.-Y. Lu, G.-X. Peng, and Y.-P. Zhao, *Nucl. Sci. Tech.* **33**, 143 (2022).
 - [7] K. Oyamatsu, I. Tanihata, Y. Sugahara, K. Sumiyoshi, and H. Toki, *Nucl. Phys. A* **634**, 3 (1998).
 - [8] B. Alex Brown, *Phys. Rev. Lett.* **85**, 5296 (2000).
 - [9] R. Furnstahl, *Nucl. Phys. A* **706**, 85 (2002).
 - [10] M. Liu, Z.-X. Li, N. Wang, and F.-S. Zhang, *Chin. Phys. C* **35**, 629 (2011).
 - [11] Z. Zhang and L.-W. Chen, *Phys. Lett. B* **726**, 234 (2013).
 - [12] J. Xu, W.-J. Xie, and B.-A. Li, *Phys. Rev. C* **102**, 044316 (2020).
 - [13] L.-G. Cao and Z.-Y. Ma, *Chin. Phys. Lett.* **25**, 1625 (2008).
 - [14] L.-G. Cao, X. Roca-Maza, G. Colò, and H. Sagawa, *Phys. Rev. C* **92**, 034308 (2015).
 - [15] X. Roca-Maza, X. Viñas, M. Centelles, B. K. Agrawal, G. Colò, N. Paar, J. Piekarewicz, and D. Vretenar, *Phys. Rev. C* **92**, 064304 (2015).
 - [16] X. Roca-Maza, L.-G. Cao, G. Colò, and H. Sagawa, *Phys. Rev. C* **94**, 044313 (2016).
 - [17] S.-H. Cheng, J. Wen, L.-G. Cao, and F.-S. Zhang, *Chin. Phys. C* **47**, 024102 (2023).
 - [18] W. Lynch, M. Tsang, Y. Zhang, P. Danielewicz, M. Famiano, Z. Li, and A. Steiner, *Prog. Part. Nucl. Phys.* **62**, 427 (2009), heavy-Ion Collisions in the Coulomb Barrier to the Quark-Gluon Plasma.
 - [19] M. D. Toro, V. Baran, M. Colonna, and V. Greco, *J. Phys. G* **37**, 083101 (2010).
 - [20] S. Kumar, Y. G. Ma, G. Q. Zhang, and C. L. Zhou, *Phys. Rev. C* **84**, 044620 (2011).
 - [21] W.-J. Xie, J. Su, L. Zhu, and F.-S. Zhang, *Phys. Lett. B* **718**, 1510 (2013).
 - [22] Z.-Q. Feng and G.-M. Jin, *Phys. Lett. B* **683**, 140 (2010).
 - [23] H. Yu, D.-Q. Fang, and Y.-G. Ma, *Nucl. Sci. Tech.* **31**, 61 (2020).
 - [24] N. Wang and T. Li, *Phys. Rev. C* **88**, 011301(R) (2013).
 - [25] B. A. Brown, *Phys. Rev. Lett.* **119**, 122502 (2017).
 - [26] B. A. Brown, K. Minamisono, J. Piekarewicz, H. Hergert, D. Garand, A. Klose, K. König, J. D. Lantis, Y. Liu, B. Maaß, A. J. Miller, W. Nörtershäuser, S. V. Pineda, R. C. Powel, D. M. Rossi, F. Sommer, C. Sumithrarachchi, A. Teigelhöfer, J. Watkins, and R. Wirth, *Phys. Rev. Res.* **2**, 022035 (2020).
 - [27] S. V. Pineda, K. König, D. M. Rossi, B. A. Brown, A. Incorvati, J. Lantis, K. Minamisono, W. Nörtershäuser, J. Piekarewicz, R. Powel, and F. Sommer, *Phys. Rev. Lett.* **127**, 182503 (2021).
 - [28] K. König *et al.*, (2023), [arXiv:2309.02037](https://arxiv.org/abs/2309.02037) [nucl-ex].
 - [29] J. Yang and J. Piekarewicz, *Phys. Rev. C* **97**, 014314 (2018).

- [30] M.-Q. Ding, P. Su, D.-Q. Fang, and S.-M. Wang, *Chin.Phys. C* **47**, 094101 (2023).
- [31] S. J. Novario, D. Lonardonì, S. Gandolfi, and G. Hagen, *Phys. Rev. Lett.* **130**, 032501 (2023).
- [32] P. Bano, S. P. Pattnaik, M. Centelles, X. Viñas, and T. R. Routray, *Phys. Rev. C* **108**, 015802 (2023).
- [33] X.-F. Yang, S.-J. Wang, S.-G. Wilkins, and R.-F. G. Ruiz, *Prog. Part. Nucl. Phys.* **129**, 104005 (2023).
- [34] I. Angeli and K. Marinova, *At. Data Nucl. Data Tables* **99**, 69 (2013).
- [35] T. Li, Y. Luo, and N. Wang, *At. Data Nucl. Data Tables* **140**, 101440 (2021).
- [36] G. Lalazissis, M. Sharma, and P. Ring, *Nucl. Phys. A* **597**, 35 (1996).
- [37] T. Togashi, Y. Tsunoda, T. Otsuka, and N. Shimizu, *Phys. Rev. Lett.* **117**, 172502 (2016).
- [38] R. An, S.-S. Zhang, L.-S. Geng, and F.-S. Zhang, *Chin. Phys. C* **46**, 054101 (2022).
- [39] R. An, X.-X. Dong, L.-G. Cao, and F.-S. Zhang, *Commun. Theor. Phys.* **75**, 035301 (2023).
- [40] P.-G. Reinhard and W. Nazarewicz, *Phys. Rev. C* **95**, 064328 (2017).
- [41] R. An, L.-S. Geng, and S.-S. Zhang, *Phys. Rev. C* **102**, 024307 (2020).
- [42] R. An, X. Jiang, L.-G. Cao, and F.-S. Zhang, *Phys. Rev. C* **105**, 014325 (2022).
- [43] H. Nakada, *Phys. Rev. C* **100**, 044310 (2019).
- [44] U. C. Perera, A. V. Afanasjev, and P. Ring, *Phys. Rev. C* **104**, 064313 (2021).
- [45] J. Meng, *Nucl. Phys. A* **635**, 3 (1998).
- [46] L.-S. Geng, H. Toki, S. Sugimoto, and J. Meng, *Prog. Theor. Phys.* **110**, 921 (2003).
- [47] R. An, L. S. Geng, S. S. Zhang, and L. Liu, *Chin. Phys. C* **42**, 114101 (2018).
- [48] Y. Zhang and X. Y. Qu, *Phys. Rev. C* **102**, 054312 (2020).
- [49] Y. Zhang, Y. Chen, J. Meng, and P. Ring, *Phys. Rev. C* **95**, 014316 (2017).
- [50] P.-G. Reinhard and W. Nazarewicz, *Phys. Rev. C* **105**, L021301 (2022).
- [51] Y. N. Huang, Z. Z. Li, and Y. F. Niu, *Phys. Rev. C* **107**, 034319 (2023).
- [52] R. An, S. Sun, L.-G. Cao, and F.-S. Zhang, (2023), [arXiv:2312.15434 \[nucl-th\]](https://arxiv.org/abs/2312.15434).
- [53] S. Yoshida and H. Sagawa, *Phys. Rev. C* **69**, 024318 (2004).
- [54] S. Yoshida and H. Sagawa, *Phys. Rev. C* **73**, 044320 (2006).
- [55] J. Xu, Z. Zhang, and B.-A. Li, *Phys. Rev. C* **104**, 054324 (2021).
- [56] D. Chatterjee, F. Gulminelli, A. R. Raduta, and J. Margueron, *Phys. Rev. C* **96**, 065805 (2017).
- [57] C. Mondal and F. Gulminelli, *Phys. Rev. C* **107**, 015801 (2023).
- [58] J. Piekarewicz, *Phys. Rev. C* **69**, 041301 (2004).
- [59] L.-W. Chen and J.-Z. Gu, *J. Phys. G* **39**, 035104 (2012).
- [60] A. Kumar, H. C. Das, and S. K. Patra, *Phys. Rev. C* **104**, 055804 (2021).
- [61] M. Bender, P.-H. Heenen, and P.-G. Reinhard, *Rev. Mod. Phys.* **75**, 121 (2003).
- [62] J. C. Pei, M. V. Stoitsov, G. I. Fann, W. Nazarewicz, N. Schunck, and F. R. Xu, *Phys. Rev. C* **78**, 064306 (2008).
- [63] J. C. Pei, Y. N. Zhang, and F. R. Xu, *Phys. Rev. C* **87**, 051302 (2013).
- [64] N. Wang, M. Liu, X. Wu, and J. Meng, *Phys. Rev. C* **93**, 014302 (2016).
- [65] X. Jiang and N. Wang, *Chin. Phys. C* **42**, 104105 (2018).
- [66] X. Y. Qu and Y. Zhang, *Phys. Rev. C* **99**, 014314 (2019).
- [67] Z. Wu and L. Guo, *Phys. Rev. C* **100**, 014612 (2019).
- [68] X. Jiang and N. Wang, *Phys. Rev. C* **101**, 014604 (2020).
- [69] X. Jiang and N. Wang, *Front. Phys.* **8** (2020), 10.3389/fphy.2020.00038.
- [70] J. C. Pei, G. I. Fann, R. J. Harrison, W. Nazarewicz, Y. Shi, and S. Thornton, *Phys. Rev. C* **90**, 024317 (2014).
- [71] Q. Z. Chai, J. C. Pei, N. Fei, and D. W. Guan, *Phys. Rev. C* **102**, 014312 (2020).
- [72] Y. Zhang, H. Sagawa, and E. Hiyama, *Phys. Rev. C* **103**, 034321 (2021).
- [73] Q. Z. Chai, Y. Qiang, and J. C. Pei, *Phys. Rev. C* **105**, 034315 (2022).
- [74] Z.-J. Wu, L. Guo, Z. Liu, and G.-X. Peng, *Phys. Lett. B* **825**, 136886 (2022).
- [75] E.-B. Huo, K.-R. Li, X.-Y. Qu, Y. Zhang, and T.-T. Sun, *Nucl. Sci. Tech.* **34**, 105 (2023).
- [76] H. Nakada, *Phys. Rev. C* **68**, 014316 (2003).
- [77] M. Dutra, O. Lourenço, J. S. Sá Martins, A. Delfino, J. R. Stone, and P. D. Stevenson, *Phys. Rev. C* **85**, 035201 (2012).
- [78] H. S. Köhler, *Nucl. Phys. A* **258**, 301 (1976).
- [79] E. Chabanat, P. Bonche, P. Haensel, J. Meyer, and R. Schaeffer, *Nucl. Phys. A* **627**, 710 (1997).
- [80] E. Chabanat, P. Bonche, P. Haensel, J. Meyer, and R. Schaeffer, *Nucl. Phys. A* **635**, 231 (1998).
- [81] J. Meng and P. Ring, *Phys. Rev. Lett.* **77**, 3963 (1996).
- [82] K. Bennaceur and J. Dobaczewski, *Comp. Phys. Commun.* **168**, 96 (2005).
- [83] L.-G. Cao, H. Sagawa, and G. Colò, *Phys. Rev. C* **86**, 054313 (2012).
- [84] Y. K. Gambhir, P. Ring, and A. Thimet, *Ann. Phys.* **198**, 132 (1990).
- [85] G. Colò, N. Van Giai, J. Meyer, K. Bennaceur, and P. Bonche, *Phys. Rev. C* **70**, 024307 (2004).
- [86] W. M. Seif, *Phys. Rev. C* **74**, 034302 (2006).
- [87] A. J. Miller, K. Minamisono, A. Klose, D. Garand, C. Kujawa, J. D. Lantis, Y. Liu, B. Maaß, P. F. Mantica, W. Nazarewicz, W. Nörtershäuser, S. V. Pineda, P.-G. Reinhard, D. M. Rossi, F. Sommer, C. Sumithrarachchi, A. Teigelhöfer, and J. Watkins, *Nature Phys.* **15**, 432 (2019).
- [88] R. An, S. Sun, L.-G. Cao, and F.-S. Zhang, *Nucl. Sci. Tech.* **34**, 119 (2023).
- [89] A. Carbone, G. Colò, A. Bracco, L.-G. Cao, P. F. Bortignon, F. Camera, and O. Wieland, *Phys. Rev. C* **81**, 041301(R) (2010).
- [90] C. A. Raithel and F. Özel, *Astrophys. J.* **885**, 121 (2019).
- [91] H.-J. Liu, H.-G. Cheng, and Z.-Q. Feng, (2023), [arXiv:2302.02131 \[nucl-th\]](https://arxiv.org/abs/2302.02131).
- [92] Z. Zhang and L.-W. Chen, *Phys. Rev. C* **90**, 064317 (2014).
- [93] M. Veselsky, J. Klimo, Y.-G. Ma, and G. A. Souliotis, *Phys. Rev. C* **94**, 064608 (2016).
- [94] C. Xu, Z. Ren, and J. Liu, *Phys. Rev. C* **90**, 064310 (2014).

- [95] S. Yang, R. Li, and C. Xu, *Phys. Rev. C* **108**, L021303 (2023).
- [96] M. Qiu, B.-J. Cai, L.-W. Chen, C.-X. Yuan, and Z. Zhang, (2023), [arXiv:2312.07031 \[nucl-th\]](https://arxiv.org/abs/2312.07031).
- [97] J.-Y. Xu, Z.-Z. Li, B.-H. Sun, Y.-F. Niu, X. Roca-Maza, H. Sagawa, and I. Tanihata, *Phys. Lett. B* **833**, 137333 (2022).
- [98] C.-J. Wang, G. Guo, H. J. Ong, Y.-N. Song, B.-H. Sun, I. Tanihata, S. Terashima, X.-L. Wei, J.-Y. Xu, X.-D. Xu, J.-C. Zhang, Y. Zheng, L.-H. Zhu, Y. Cao, G.-W. Fan, B.-S. Gao, J.-X. Han, G.-S. Li, C.-G. Lu, H.-T. Qi, Y. Qin, Z.-Y. Sun, L.-P. Wan, K.-L. Wang, S.-T. Wang, X.-X. Wang, M.-X. Zhang, W.-W. Zhang, X.-B. Zhang, X.-H. Zhang, and Z.-C. Zhou, *Chin. Phys. C* **47**, 084001 (2023).
- [99] J. Zhao, B.-H. Sun, I. Tanihata, S. Terashima, A. Proc-hazka, J. Xu, L. Zhu, J. Meng, J. Su, K. Zhang, L. Geng, L. He, C. Liu, G. Li, C. Lu, W. Lin, W. Lin, Z. Liu, P. Ren, Z. Sun, F. Wang, J. Wang, M. Wang, S. Wang, X. Wei, X. Xu, J. Zhang, M. Zhang, and X. Zhang, *Phys. Lett. B* **847**, 138269 (2023).
- [100] B. H. Sun, Y. Lu, J. P. Peng, C. Y. Liu, and Y. M. Zhao, *Phys. Rev. C* **90**, 054318 (2014).
- [101] M. Bao, Y. Lu, Y. M. Zhao, and A. Arima, *Phys. Rev. C* **94**, 064315 (2016).
- [102] M. Bao, Y. Y. Zong, Y. M. Zhao, and A. Arima, *Phys. Rev. C* **102**, 014306 (2020).
- [103] C. Ma, Y. Y. Zong, Y. M. Zhao, and A. Arima, *Phys. Rev. C* **104**, 014303 (2021).
- [104] Y. Qian, Z. Ren, and D. Ni, *Phys. Rev. C* **89**, 024318 (2014).
- [105] D. Ni, Z. Ren, T. Dong, and Y. Qian, *Phys. Rev. C* **87**, 024310 (2013).